



Measurement of the Charged Particle Multiplicity Distribution in Hadronic Z Decays

The ALEPH Collaboration

Abstract

The charged particle multiplicity distribution of hadronic Z decays was measured on the peak of the Z resonance using the ALEPH detector at LEP. Using a model independent unfolding procedure the distribution was found to have a mean $\langle n \rangle = 20.85 \pm 0.24$ and a dispersion $D = 6.34 \pm 0.12$. Comparison with lower energy data supports the KNO scaling hypothesis in the energy range $\sqrt{s} = 29 - 91.25$ GeV. At $\sqrt{s} = 91.25$ GeV the shape of the multiplicity distribution is well described by a log-normal distribution, as predicted from a cascading model for multi-particle production. The same model also successfully describes the energy dependence of the mean and width of the multiplicity distribution. A next-to-leading order QCD prediction in the framework of the modified leading-log approximation and local parton-hadron duality is found to fit the energy dependence of the mean but not the width of the charged multiplicity distribution, indicating that the width of the multiplicity distribution is a sensitive probe for higher order QCD or non-perturbative effects.

submitted to Physics Letters B

The ALEPH Collaboration

D. Decamp, B. Deschizeaux, C. Goy, J.-P. Lees, M.-N. Minard

Laboratoire de Physique des Particules (LAPP), IN²P³-CNRS, 74019 Annecy-le-Vieux Cedex, France

R. Alemany, J.M. Crespo, M. Delfino, E. Fernandez, V. Gaitan, Ll. Garrido, Ll.M. Mir, A. Pacheco

Laboratorio de Fisica de Altas Energias, Universidad Autonoma de Barcelona, 08193 Bellaterra (Barcelona), Spain⁸

M.G. Catanesi, D. Creanza, M. de Palma, A. Farilla, G. Iaselli, G. Maggi, M. Maggi, S. Natali, S. Nuzzo, M. Quattromini, A. Ranieri, G. Raso, F. Romano, F. Ruggieri, G. Selvaggi, L. Silvestris, P. Tempesta, G. Zito

INFN Sezione di Bari e Dipartimento di Fisica dell' Universita', 70126 Bari, Italy

Y. Gao, H. Hu,²¹ D. Huang, X. Huang, J. Lin, J. Lou, C. Qiao,²¹ T. Ruan,²¹ T. Wang, Y. Xie, D. Xu, R. Xu, J. Zhang, W. Zhao

Institute of High-Energy Physics, Academia Sinica, Beijing, The People's Republic of China⁹

W.B. Atwood,² L.A.T. Bauerdick, F. Bird,⁴ E. Blucher, G. Bonvicini, F. Bossi, J. Boudreau, T.H. Burnett,³ H. Drevermann, R.W. Forty, C. Grab,²³ R. Hagelberg, S. Haywood, J. Hilgart, B. Jost, M. Kasemann,²⁸ J. Knobloch, A. Lacourt, E. Lançon, I. Lehraus, T. Lohse, A. Lusiani, A. Marchioro, M. Martinez, P. Mato, S. Menary,²⁹ T. Meyer, A. Minten, A. Miotto, R. Miquel, H.-G. Moser, J. Nash, P. Palazzi, F. Ranjard, G. Redlinger, L. Rolandi,³⁰ A. Roth, J. Rothberg,³ H. Rotscheidt, M. Saich, D. Schlatter, M. Schmelling, W. Tejessy, H. Wachsmuth, S. Wasserbaech, W. Wiedenmann, W. Witzeling, J. Wotschack

European Laboratory for Particle Physics (CERN), 1211 Geneva 23, Switzerland

Z. Ajaltouni, F. Badaud, M. Bardadin-Otwinowska, A.M. Bencheikh, R. El Fellous, A. Falvard, P. Gay, C. Guicheney, P. Henrard, J. Jousset, B. Michel, J.-C. Montret, D. Pallin, P. Perret, J. Proriol, F. Prulhière, G. Stimpfl

Laboratoire de Physique Corpusculaire, Université Blaise Pascal, IN²P³-CNRS, Clermont-Ferrand, 63177 Aubière, France

J.D. Hansen, J.R. Hansen, P.H. Hansen, R. Møllerud, B.S. Nilsson

Niels Bohr Institute, 2100 Copenhagen, Denmark¹⁰

I. Efthymiopoulos, E. Simopoulou, A. Vayaki

Nuclear Research Center Demokritos (NRCD), Athens, Greece

J. Badier, A. Blondel, G. Bonneaud, J.C. Brient, G. Fouque, A. Gamess, J. Harvey, S. Orteu, A. Rosowsky, A. Rougé, M. Rumpf, R. Tanaka, H. Videau

Laboratoire de Physique Nucléaire et des Hautes Energies, Ecole Polytechnique, IN²P³-CNRS, 91128 Palaiseau Cedex, France

D.J. Candlin, E. Veitch

Department of Physics, University of Edinburgh, Edinburgh EH9 3JZ, United Kingdom¹¹

L. Moneta, G. Parrini

Dipartimento di Fisica, Università di Firenze, INFN Sezione di Firenze, 50125 Firenze, Italy

M. Corden, C. Georgiopoulos, M. Ikeda, J. Lannutti, D. Levinthal,¹⁶ M. Mermikides, L. Sawyer

Supercomputer Computations Research Institute and Dept. of Physics, Florida State University, Tallahassee, FL 32306, USA^{13,14,15}

A. Antonelli, R. Baldini, G. Bencivenni, G. Bologna,⁵ P. Campana, G. Capon, F. Cerutti, V. Chiarella, B. D'Ettorre-Piazzoli,⁶ G. Felici, P. Laurelli, G. Mannocchi,⁶ F. Murtas, G.P. Murtas, L. Passalacqua, M. Pepe-Altarelli, P. Picchi,⁵ P. Zografou

Laboratori Nazionali dell'INFN (LNF-INFN), 00044 Frascati, Italy

B. Altoon, O. Boyle, P. Colrain, A.W. Halley, I. ten Have, J.G. Lynch, W. Maitland, W.T. Morton, C. Raine, J.M. Scarr, K. Smith, A.S. Thompson, R.M. Turnbull

Department of Physics and Astronomy, University of Glasgow, Glasgow G12 8QQ, United Kingdom¹¹

B. Brandl, O. Braun, R. Geiges, C. Geweniger, P. Hanke, V. Hepp, E.E. Kluge, Y. Maumary, A. Putzer, B. Rensch, A. Stahl, K. Tittel, M. Wunsch

Institut für Hochenergiephysik, Universität Heidelberg, 6900 Heidelberg, Fed. Rep. of Germany¹⁷

A.T. Belk, R. Beuselinck, D.M. Binnie, W. Cameron, M. Cattaneo, P.J. Dornan,¹ S. Dugeay, A.M. Greene, J.F. Hassard, N.M. Lieske, S.J. Patton, D.G. Payne, M.J. Phillips, J.K. Sedgbeer, G. Taylor, I.R. Tomalin, A.G. Wright

Department of Physics, Imperial College, London SW7 2BZ, United Kingdom¹¹

P. Girtler, D. Kuhn, G. Rudolph

Institut für Experimentalphysik, Universität Innsbruck, 6020 Innsbruck, Austria¹⁹

C.K. Bowdery, T.J. Brodbeck, A.J. Finch, F. Foster, G. Hughes, N.R. Keemer, M. Nuttall, A. Patel, B.S. Rowlingson, T. Sloan, S.W. Snow, E.P. Whelan

Department of Physics, University of Lancaster, Lancaster LA1 4YB, United Kingdom¹¹

T. Barczewski, K. Kleinknecht, J. Raab, B. Renk, S. Roehn, H.-G. Sander, H. Schmidt, F. Steeg, S.M. Walther, B. Wolf

Institut für Physik, Universität Mainz, 6500 Mainz, Fed. Rep. of Germany¹⁷

J.-J. Aubert, C. Benchouk, V. Bernard, A. Bonissent, J. Carr, P. Coyle, J. Drinkard, F. Etienne, S. Papalexioiu, P. Payre, B. Pietrzyk, Z. Qian, D. Rousseau, P. Schwemling, M. Talby

Centre de Physique des Particules, Faculté des Sciences de Luminy, IN²P³-CNRS, 13288 Marseille, France

S. Adlung, H. Becker, W. Blum, D. Brown, P. Cattaneo,³¹ G. Cowan, B. Dehning, H. Dietl, F. Dydak,²⁶ M. Fernandez-Bosman, T. Hansl-Kozanecka,^{2,22} A. Jahn, W. Kozanecki,² E. Lange, J. Lauber, G. Lütjens, G. Lutz, W. Männer, Y. Pan, R. Richter, J. Schröder, A.S. Schwarz, R. Settles, U. Stierlin, R. St. Denis, M. Takashima, J. Thomas, G. Wolf

Max-Planck-Institut für Physik und Astrophysik, Werner-Heisenberg-Institut für Physik, 8000 München, Fed. Rep. of Germany¹⁷

V. Bertin, J. Boucrot, O. Callot, X. Chen, A. Cordier, M. Davier, J.-F. Grivaz, M.-H. Gros, Ph. Heusse, P. Janot, D.W. Kim,²⁰ F. Le Diberder, J. Lefrançois,¹ A.-M. Lutz, J.-J. Veillet, I. Videau, Z. Zhang, F. Zomer

Laboratoire de l'Accélérateur Linéaire, Université de Paris-Sud, IN²P³-CNRS, 91405 Orsay Cedex, France

D. Abbaneo, S.R. Amendolia, G. Bagliesi, G. Batignani, L. Bosisio, U. Bottigli, C. Bradaschia, M. Carpinelli, M.A. Ciocci, R. Dell'Orso, I. Ferrante, F. Fidecaro,¹ L. Foà, E. Focardi, F. Forti, C. Gatto, A. Giassi, M.A. Giorgi, F. Ligabue, E.B. Mannelli, P.S. Marrocchesi, A. Messineo, F. Palla, G. Sanguinetti, J. Steinberger, R. Tenchini, G. Tonelli, G. Triggiani, C. Vannini, A. Venturi, P.G. Verdini, J. Walsh

Dipartimento di Fisica dell'Università, INFN Sezione di Pisa, e Scuola Normale Superiore, 56010 Pisa, Italy

J.M. Carter, M.G. Green,¹ P.V. March, T. Medcalf, I.S. Quazi, J.A. Strong, L.R. West, T. Wildish

Department of Physics, Royal Holloway & Bedford New College, University of London, Surrey TW20 OEX, United Kingdom¹¹

D.R. Botterill, R.W. Clift, T.R. Edgecock, M. Edwards, S.M. Fisher, T.J. Jones, P.R. Norton, D.P. Salmon, J.C. Thompson

Particle Physics Dept., Rutherford Appleton Laboratory, Chilton, Didcot, Oxon OX11 0QX, United Kingdom¹¹

B. Bloch-Devaux, P. Colas, E. Locci, S. Loucatos, E. Monnier, P. Perez, J.A. Perlas, F. Perrier, J. Rander, J.-F. Renardy, A. Roussarie, J.-P. Schuller, J. Schwindling, B. Vallage

Département de Physique des Particules Élémentaires, CEN-Saclay, 91191 Gif-sur-Yvette Cedex, France¹⁸

J.G. Ashman, C.N. Booth, C. Buttar, R.E. Carney, S. Cartwright, F. Combley, M. Dogru, F. Hatfield, J. Martin, D. Parker, P. Reeves, L.F. Thompson

Department of Physics, University of Sheffield, Sheffield S3 7RH, United Kingdom¹¹

E. Barberio, S. Brandt, C. Grupen, H. Meinhard, L. Mirabito, U. Schäfer, H. Seywerd

Fachbereich Physik, Universität Siegen, 5900 Siegen, Fed. Rep. of Germany¹⁷

G. Ganis, G. Giannini, B. Gobbo, F. Ragusa,²⁵U. Stiegler

Dipartimento di Fisica, Università di Trieste e INFN Sezione di Trieste, 34127 Trieste, Italy

L. Bellantoni, D. Cinabro, J.S. Conway, D.F. Cowen,²⁴ Z. Feng, D.P.S. Ferguson, Y.S. Gao, J. Grahl, J.L. Harton, R.C. Jared,⁷ R.P. Johnson,²⁷ B.W. LeClaire, C. Lishka, Y.B. Pan, J.R. Pater, Y. Saadi, V. Sharma, Z.H. Shi, Y.H. Tang, A.M. Walsh, J.A. Wear,²⁷ F.V. Weber, M.H. Whitney, Sau Lan Wu, G. Zoebnig

Department of Physics, University of Wisconsin, Madison, WI 53706, USA¹²

¹Now at CERN.

²Permanent address: SLAC, Stanford, CA 94309, USA.

³Permanent address: University of Washington, Seattle, WA 98195, USA.

⁴Now at SSCL, Dallas, TX, U.S.A.

⁵Also Istituto di Fisica Generale, Università di Torino, Torino, Italy.

⁶Also Istituto di Cosmo-Geofisica del C.N.R., Torino, Italy.

⁷Permanent address: LBL, Berkeley, CA 94720, USA.

⁸Supported by CAICYT, Spain.

⁹Supported by the National Science Foundation of China.

¹⁰Supported by the Danish Natural Science Research Council.

¹¹Supported by the UK Science and Engineering Research Council.

¹²Supported by the US Department of Energy, contract DE-AC02-76ER00881.

¹³Supported by the US Department of Energy, contract DE-FG05-87ER40319.

¹⁴Supported by the NSF, contract PHY-8451274.

¹⁵Supported by the US Department of Energy, contract DE-FC05-85ER250000.

¹⁶Supported by SLOAN fellowship, contract BR 2703.

¹⁷Supported by the Bundesministerium für Forschung und Technologie, Fed. Rep. of Germany.

¹⁸Supported by the Institut de Recherche Fondamentale du C.E.A.

¹⁹Supported by Fonds zur Förderung der wissenschaftlichen Forschung, Austria.

²⁰Supported by the Korean Science and Engineering Foundation and Ministry of Education.

²¹Supported by the World Laboratory.

²²On leave of absence from MIT, Cambridge, MA 02139, USA.

²³Now at ETH, Zürich, Switzerland.

²⁴Now at California Institute of Technology, Pasadena, CA 91125, USA.

²⁵Now at Dipartimento di Fisica, Università di Milano, Milano, Italy.

²⁶Also at CERN, PPE Division, 1211 Geneva 23, Switzerland.

²⁷Now at University of California, Santa Cruz, CA 95064, USA.

²⁸Now at DESY, Hamburg, Germany.

²⁹Now at Cornell University, Ithaca, NY 14853, USA.

³⁰Also at Dipartimento di Fisica, Università di Trieste, Trieste, Italy.

³¹Now at INFN, Pavia, Italy.

1 Introduction

The properties of hadronic Z decays are well understood within the framework of perturbative QCD and phenomenological fragmentation models. A complete understanding of the dynamics of multi-particle production, however, is still lacking. One particularly simple observable, which contains information about the dynamics of hadron production, is the charged particle multiplicity distribution. A number of models [1, 2, 3, 4] make predictions for the evolution of the shape and the leading moments of the multiplicity distribution as a function of the centre-of-mass energy \sqrt{s} . The successful operation of the Large Electron Positron Collider at CERN allows a test of these predictions up to $\sqrt{s} = 91.25$ GeV.

The charged particle multiplicity distribution is presented for a sample of 90000 hadronic Z decays at $\sqrt{s} = M_Z$ measured with the ALEPH detector at LEP in 1989 and 1990. The paper is organized as follows: section 2 contains a brief summary of the data analysis, in section 3 the procedure for unfolding the data is described and in section 4 the model independent results obtained for the charged particle multiplicity distribution are presented. Parametric models for the shape and energy dependence of the multiplicity distribution are discussed in sections 5 and 6, respectively. Section 7 summarizes the results.

2 Data analysis

Details of the ALEPH detector and the trigger are described elsewhere [5]. For hadronic Z decays the trigger efficiency was found to be effectively 100%. Here the detector components relevant to this analysis are reviewed. The momenta of charged particles are measured in two central tracking chambers. The inner tracking chamber (ITC) is a conventional drift chamber which provides up to 8 coordinates per track. The outer chamber, a large time projection chamber (TPC) of radius 1.8 m, yields up to 21 additional space points per track. The single coordinate resolution of the TPC is typically 1.2 mm in z and $170 \mu\text{m}$ in $r\phi$. Both chambers are located inside a superconducting solenoid. A momentum resolution of $\Delta p/p^2 = 0.0008$ (GeV/c) $^{-1}$ is achieved by the combined system of TPC and ITC.

An event was accepted as hadronic if it had at least five charged tracks, a total charged energy in excess of 15 GeV, and if the polar angle of the sphericity axis was in the range $35^\circ \leq \theta_{sph} \leq 145^\circ$. Each track was required to have at least 4 coordinates in the TPC and to originate from a cylindrical region with a radius $d_0 = 3$ cm and length $z_0 = 5$ cm around the interaction point. In addition, the transverse momentum p_T with respect to the beam axis had to be larger than 200 MeV/c and the polar angle to the beam direction between 20° and 160° .

The true charged multiplicity of an event was defined as the number of charged tracks that is obtained if all particles with a mean lifetime $\tau \leq 1$ nanosecond decay while the others are stable. Thus, charged decay products of K_s^0 's and strange baryons are included. Apart from decay corrections the measured charged multiplicity of an event can differ from that defined above due to acceptance losses or secondary interactions of particles with detector material.

The relation between the observed multiplicity distribution, O_i , $i = 1, 2, 3, \dots$, and the underlying true distribution, T_j , $j = 2, 4, 6, \dots$, can be described by a matrix equation [6]:

$$O_i = \sum_j G_{ij} \cdot T_j . \quad (1)$$

This has to be inverted in order to extract the true distribution from the data. Each element of the response matrix G_{ij} is the product of the probability that a true multiplicity j will be reconstructed as multiplicity i , times the probability that an event with true charged multiplicity j survives the event selection criteria. This matrix was determined from a Monte Carlo simulation of hadronic events which

included the complete chain of detector simulation, reconstruction and analysis programs, based on 53000 hadronic Z decays generated with the Lund parton shower model [7].

The raw response matrix as estimated from the Monte Carlo simulation was parametrized by a smooth function in order to avoid spurious structures in the corrected multiplicity distribution that are due to statistical fluctuations in the response matrix. Figure 1 shows some slices of the response matrix and how the parametrization compares to the Monte Carlo simulation. The uncertainty associated with the smoothing procedure is allowed for in the systematic errors of the results. By construction the response matrix G for a given Monte Carlo generator is independent of the relative frequencies of events with a fixed true charged multiplicity. Therefore it is only very weakly dependent on the actual choice of the event generator. Using e.g. the Lund 6.3 matrix element generator [8] with default parameter values, which is known to give a worse description of the LEP data, the change in the results turns out to be negligible.

The raw charged multiplicity distribution was corrected for $e^+e^- \rightarrow \tau^+\tau^-$ events which constitute the dominant background from non-hadronic Z -decays. They contribute to measured multiplicities from 5 to 7 tracks and amount to roughly 0.27 % of the accepted events.

3 The Unfolding Procedure

Because of charge conservation the true charged multiplicity of an event is always even-valued while observed multiplicities also can be odd-valued. One might use this constraint to solve equation (1) for the true distribution \mathbf{T} by a least squares fit. However, this approach yields unstable results: small statistical fluctuations in the observed distributions result in radically different estimates of the shape of the true distributions. Intuitively this can be understood from the fact that r.m.s. width of the difference between the true and the observed multiplicity of an event is ≈ 2.6 units. The information about one specific bin of the true multiplicity distribution thereby is smeared out over so many bins of the observed one, that at finite statistics the true distribution is effectively underconstrained by the measurements.

A widely used alternative, see e.g. reference [9], to bypass the problems connected with the inversion of equation (1) is to estimate directly from the Monte Carlo simulation a probability matrix p_{ij} that an event with measured multiplicity i has a true multiplicity j . The corrected distribution is then obtained by multiplying the measured distribution with this matrix: $T_j = \sum_i p_{ij} O_i$. However, since these probabilities depend crucially on the multiplicity distribution put into the simulation, the unfolding result obtained that way is biased towards the input of the Monte Carlo. This model dependence is avoided when solving the inverse problem eq. (1).

One approach to estimate a probability distribution which is not uniquely defined by a set of constraints is given by the ‘‘Method of Maximum Entropy’’ (MME) [10]. For underconstrained problems this is known to be the only method of inference which satisfies elementary requirements of consistency [11]. The ‘‘Method of Reduced Entropy’’ (MRE) [12, 13] employed in this analysis is a generalization of the MME. It takes into account the fact that the constraints obtained from experimental data are subject to statistical fluctuations by combining the principle of maximum entropy with the least squares method. The unfolded multiplicity distribution \mathbf{T} is obtained by minimizing

$$F = w\chi^2 - S \quad (2)$$

with: w : regularization parameter $w > 0$
 χ^2 : $(\mathbf{O} - G\mathbf{T})^T C^{-1}(\mathbf{O} - G\mathbf{T})$
 C : covariance matrix of the measured distribution \mathbf{O}
 S : information entropy of the true distribution \mathbf{T}

$$S = - \sum_i p_i \log(p_i) \quad p_i = T_i / \sum_k T_k.$$

The constant w ¹ determines the relative weight of the measurements (χ^2) with respect to the smoothing term (S).

4 Model Independent Results

The unfolded charged multiplicity distribution of hadronic Z decays is shown in Figure 2(a) and the probabilities are given in table 1. Note that due to the correction procedure the errors are correlated. Since the selection criteria require at least 5 observed charged tracks per event there is no information about the probability of having a hadronic Z decay with only two charged tracks. The respective entry in table 1 is the expectation from the Lund 7.2 parton shower model. Because of smearing the probability for a Z to produce 4 charged tracks can still be estimated, albeit with large errors. Table 2 contains the results for the mean charged multiplicity $\langle n \rangle$, dispersion D where

$$D = \sqrt{\langle n^2 \rangle - \langle n \rangle^2},$$

and the derived quantities $\langle n \rangle / D$ and second binomial moment R_2 , where

$$R_2 = \frac{\langle n(n-1) \rangle}{\langle n \rangle^2} = 1 + \frac{D^2}{\langle n \rangle^2} - \frac{1}{\langle n \rangle}.$$

The systematic errors given in table 2 cover uncertainties due to:

- Finite Monte Carlo statistics and the smoothing procedure. The latter contribution was estimated by the difference found when fitting the multiplicity distribution either with the smoothed response matrix or with the raw matrix.
- Dependencies on the event generator and uncertainties in the simulation of the detector response. This uncertainty was taken to be the r.m.s. spread in the results, when using response matrices calculated with different event generators and different versions of the detector simulation and reconstruction program.

Additional contributions to the systematic errors are related to the following uncertainties in the mean charged particle multiplicity:

- Uncertainties in the multiplicity of tracks with p_T below 0.2 GeV/c which are not measured. This loss amounts to 1.9 units. A comparison of the expectation from a tuned Lund parton shower model [14] and the HERWIG Monte Carlo [15] gives a difference of 0.1 tracks per event, which is taken to be the systematic error in the extrapolation $p_T \rightarrow 0$.
- The systematic error due to photon conversions. According to the Monte Carlo simulation an average of 0.5 tracks/event from photon conversions are accepted by the event selection cuts. Since the actual number of conversions in the data is about 20% larger than expected from the simulation an additional uncertainty of 0.1 tracks/event is assumed.

¹The value of w is determined such that:

$$\text{Tr}[(wS'' + S' S'^T)(1 - \frac{1}{2w}CS'')^{-2}C] = 0$$

with S' the gradient vector and S'' the second derivative matrix of S with respect to \mathbf{T} . This condition ensures that the unfolded distribution \mathbf{T} has no structural bias due to the statistical fluctuations in the information used to estimate \mathbf{T} . For more details see reference [12].

n	P_n			
*2	0.00001	±	0.00001	
4	0.00002	±	0.00020	± 0.00030
6	0.0027	±	0.0007	± 0.0012
8	0.0076	±	0.0011	± 0.0017
10	0.0291	±	0.0020	± 0.0039
12	0.0490	±	0.0033	± 0.0050
14	0.0918	±	0.0049	± 0.0083
16	0.1110	±	0.0063	± 0.0088
18	0.1328	±	0.0069	± 0.0095
20	0.1220	±	0.0064	± 0.0086
22	0.1136	±	0.0056	± 0.0075
24	0.0990	±	0.0050	± 0.0068
26	0.0789	±	0.0044	± 0.0062
28	0.0558	±	0.0035	± 0.0054
30	0.0378	±	0.0028	± 0.0043
32	0.0269	±	0.0023	± 0.0033
34	0.0196	±	0.0020	± 0.0028
36	0.0109	±	0.0014	± 0.0023
38	0.0047	±	0.0010	± 0.0016
40	0.00235	±	0.00064	± 0.00091
42	0.00210	±	0.00059	± 0.00078
44	0.00180	±	0.00061	± 0.00085
46	0.00046	±	0.00031	± 0.00059
48	0.00003	±	0.00010	± 0.00015
50	0.00000	±	0.00002	± 0.00002

Table 1: Unfolded charged particle multiplicity distribution giving the probability P_n to have a hadronic Z decay with n charged particles. The first error is the statistical error, the second the systematic uncertainty of the results. The entry for $n = 2$ is from the Lund 7.2 parton shower model.

- Decay products from K^0 's and strange baryons are accepted with an efficiency of $\approx 65\%$. The production rate for V^0 's is found to be the same in data and Monte Carlo simulation within errors, giving an average of 1.9 tracks per event, 0.7 of which are lost. Assuming an error of 10% in this simulation yields an additional uncertainty of 0.07 tracks per event.
- The relative error of 10^{-3} on the drift velocity of the TPC gives an uncertainty of 0.03 tracks/event due to the corresponding error in the definition of the cut on the polar angle of a track.
- Conservatively assuming a scale uncertainty of 5 MeV/c for the p_T cutoff of 200 MeV/c results in a systematic error of 0.08 tracks/event.
- Similarly, a systematic error of 1mm both in the setting of the z_0 and the d_0 cut in the track selection criteria translate to errors in the charged particle multiplicity of 0.01 and 0.03 tracks/event respectively.
- From a detailed study of tracking efficiency and dE/dx it is found that, due to the finite two-track resolution of the ALEPH TPC, on average 0.11 tracks are lost per hadronic event. These losses are simulated in the Monte Carlo to better than 40%, which results in a systematic error on the mean charged multiplicity of 0.04 units.

$\langle n \rangle$	=	20.85	±	0.02	±	0.24
D	=	6.34	±	0.02	±	0.11
$\langle n \rangle / D$	=	3.29	±	0.01	±	0.06
R_2	=	1.0444	±	0.0006	±	0.0032

Table 2: Leading moments of the charged particle multiplicity distribution. The first error is the statistical error, the second the systematic error on the result.

The systematic error on the mean charged particle multiplicity due to these sources amounts to 0.18 tracks/events. Assuming that this corresponds to an average of 0.09 track pairs per event fluctuating according to Poisson statistics this error on $\langle n \rangle$ was translated into a systematic error for the higher moments and the individual bins of the unfolded distribution.

5 Parametric Models

Several parametrizations for the shape of the charged particle multiplicity distribution are discussed in the literature. Here we concentrate on two:

- the log-normal (LND) distribution, and
- the negative binomial (NBD) distribution.

The log-normal distribution can be derived from the general assumption that multi-particle production proceeds via a scale invariant stochastic branching process [3, 4]. Here the discrete probability distribution is defined through

$$P_n(\mu, \sigma, c) = \int_n^{n+1} \frac{N}{n' + c} \exp\left(-\frac{[\ln(n' + c) - \mu]^2}{2\sigma^2}\right) dn'.$$

For a fit of the shape a better parametrization is obtained by expressing σ^2 and μ through

$$\sigma^2 = \ln\left(1 + \frac{d^2}{(\bar{n} + c)^2}\right) \quad \text{and} \quad \mu = \ln \frac{(\bar{n} + c)^2}{\sqrt{d^2 + (\bar{n} + c)^2}}.$$

In the limit $\mu - \ln c \gg \sigma$ the new parameters \bar{n} and d can be identified as the mean and the rms-width of the continuous distribution, which for this measurement of the charged particle multiplicity distribution turns out to be an excellent approximation. In this case \bar{n} and the mean value $\langle n \rangle$ of the discrete distribution P_n are related through $\bar{n} \approx \langle n \rangle + 0.5$.

The negative binomial distribution, first introduced as a parametrization for the multiplicity distribution by the UA5 collaboration [16], is of special interest because in a next-to-leading order QCD calculation [2] in the framework of the modified-leading-log approximation (MLLA) and local parton-hadron duality (LPHD) the moments of the multiplicity distribution are found to be approximately like those of a NBD. The distribution is given by:

$$P_n(\langle n \rangle, k) = \frac{k(k+1)\dots(k+n-1)}{n!} \left(\frac{\langle n \rangle}{\langle n \rangle + k}\right)^n \left(1 + \frac{\langle n \rangle}{k}\right)^{-k}$$

The parameters for both distributions are obtained from a least squares fit to the measurements, minimizing the χ^2 -function defined in eq. 2. The results are summarized in table 3. Figure 2(a) shows

both parametrizations with the unfolded multiplicity distribution. Figure 2(b) presents the raw data and all three estimates for the corrected distribution after convolution with the response matrix. The overall agreement is found to be quite good in all cases. For a detailed comparison the residuals between fit and data are plotted separately in Figures 2(c-e) for the unfolded distribution (c) and the parametric models LND (d) and NBD (e). The errors shown are always the purely statistical errors of the data. Here the log-normal distribution is found to give a significantly better description of the data than the negative binomial distribution. Similar observations hold for all alternative response matrices considered in the analysis. With the present understanding of the systematic uncertainties, however, the NBD is still compatible with the data.

Distribution	Parameter			
LND	\bar{n}	=	21.34	± 0.02 ± 0.24
	d	=	6.35	± 0.02 ± 0.14
	c	=	12.30	± 0.77 ± 4.29
NBD	$\langle n \rangle$	=	20.83	± 0.02 ± 0.23
	k	=	22.68	± 0.29 ± 1.33

Table 3: Parameters obtained from fits of the charged multiplicity distribution by a negative-binomial distribution (NBD) and a log-normal distribution (LND). The first error is purely statistical and the second systematic.

6 Energy Dependence of the Charged Multiplicity Distribution

6.1 KNO scaling

Originally derived starting from the Feynman scaling [17] behaviour for multi-particle production the KNO [1] scaling hypothesis predicts that the shape of the multiplicity distribution plotted in the form $\langle n \rangle P_n$ versus $z = n/\langle n \rangle$ is independent of \sqrt{s} . In Figure 3(a) the multiplicity distribution plotted in the KNO form is compared to data at $\sqrt{s} = 43.6$ GeV and $\sqrt{s} = 29$ GeV measured by the TASSO and HRS collaborations [9, 18]. It can be seen that in the energy range $\sqrt{s} = 29 - 91.25$ GeV the data are in remarkable agreement with the expectations from KNO scaling. Also shown is the distribution from Lund 7.2 parton shower model, tuned at $\sqrt{s} = 91.25$ GeV [14], which provides a very good description of the data. KNO-scaling further implies the ratio $\langle n \rangle / D$ to be independent of \sqrt{s} . Measurements of this ratio between 12 GeV and 91.25 GeV [9, 19, 20] are shown in Figure 3(b). The data are well described by a constant with $C_{KNO} = 3.23 \pm 0.05$ with a $\chi^2/NDF = 5.0/8$. The energy dependence of $\langle n \rangle / D$ is also found to be well reproduced by the Lund model without retuning parameters, i.e. approximate KNO scaling appears to be a natural consequence of the parton shower approach to multi-particle production.

6.2 The Mean Charged Multiplicity

Combining our results with data from other experiments [9, 19, 20, 21] above the $b\bar{b}$ production threshold we compare the energy dependence of $\langle n \rangle$ with expectations from three different models. A simple phenomenological ansatz similar to that given in reference [22]

$$\langle n(s) \rangle = n_0 \ln^2\left(\frac{s}{4m_\pi^2}\right)$$

already gives a good description of the data with $n_0 = 0.1525 \pm 0.0011$ and a $\chi^2/NDF = 10.1/13$.

The approach which gives rise to a log-normal distribution [4] for the shape relates the mean charged multiplicities at different centre-of-mass energies through

$$\langle n(s) \rangle = (1 + \langle n(s_0) \rangle) \left(\frac{s}{s_0} \right)^\gamma - 1.$$

Setting $\sqrt{s_0} = 91.25$ GeV and $\langle n(s_0) \rangle = 20.85$ a best fit exponent $\gamma = 0.204 \pm 0.005$ is found with a $\chi^2/NDF = 2.1/12$.

Finally, as a consequence of the running of the strong coupling constant α_s , a next-to-leading order QCD calculation [23] (MLLA+LPHD) predicts an energy dependence of the form

$$\langle n(s) \rangle = a\alpha_s^{b_1} \exp\left(\frac{b_2}{\sqrt{\alpha_s}}\right).$$

The free parameters are the normalization constant a which cannot be calculated perturbatively and a scale parameter Λ_{LLA} that governs the running of α_s . Note that Λ_{LLA} needs not to be identical to $\Lambda_{\overline{MS}}$ even though both are expected to be of the same order of magnitude. The parameters b_1 and b_2 are fixed within QCD; for five active flavours $b_1 = 0.4916$ and $b_2 = 2.265$. Taking the two loop formula for the running coupling constant [24] with the QCD-scale fixed to $\Lambda_{LLA} = 0.145$ GeV which gives $\alpha_s(M_z^2) = 0.117$ [25], the normalization constant is determined to $a = 0.0677 \pm 0.0005$ with a $\chi^2/NDF = 2.1/13$. Figure 4 shows how the fits compare to the data. Also shown is the prediction from the Lund 7.2 parton shower model with parameters fixed at $\sqrt{s} = 91$ GeV [14] which follows the QCD-curve very closely.

6.3 The Width of the Multiplicity Distribution

The cascading model that leads to the log-normal multiplicity distribution and the QCD calculation both yield predictions for the energy dependence of the width of the charged particle multiplicity distribution. The ratio $(\langle n \rangle + 0.5)/D$ is expected to be a constant for the log-normal distribution. The QCD calculation predicts the second binomial moment R_2 to behave like

$$R_2 = \frac{11}{8} [1 - \kappa\sqrt{\alpha_s}]$$

with $\kappa = 0.55$ for five flavours [2].

The ratio $\langle n \rangle / D$ was found to be constant within errors; since $\langle n \rangle$ is much larger than D also the ratio $(\langle n \rangle + 0.5)/D$ is found to be compatible with a constant $C_{LND} = 3.33 \pm 0.05$ with $\chi^2/NDF = 3.2/8$. The experimental values for R_2 are compared with the QCD prediction (MLLA+LPHD) in Figure 5. For QCD the leading and next-to-leading order predictions are plotted, with α_s again calculated according to the two loop formula [24] and the scale parameter set to $\Lambda_{LLA} = 0.145$ GeV. Both curves are significantly above the data. A best fit of the scale parameter (not shown) yields $\Lambda_{LLA} = 1.93 \pm 0.12$ GeV with $\chi^2/NDF = 38.1/8$ which is incompatible with the QCD-prediction for the energy dependence of the mean charged multiplicity. We therefore conclude that higher than next-to-leading order QCD contributions or non-perturbative effects are needed to explain the width of the charged particle multiplicity distribution, even though it is remarkable to what extent already the next-to-leading order corrections do account for the bulk of the higher order effects. The Lund 7.2 parton shower model again provides an accurate description of the measurements between $\sqrt{s} = 12 - 91.25$ GeV.

7 Summary

We have measured the charged particle multiplicity distribution in hadronic Z decays. The mean and the dispersion of the distribution are $\langle n \rangle = 20.85 \pm 0.24$ and $D = 6.34 \pm 0.12$, with $\langle n \rangle / D = 3.29 \pm 0.06$

and the second binomial moment $R_2 = 1.0444 \pm 0.0033$. The errors are the combined statistical and systematic uncertainties. The shape of the multiplicity distribution is found to be well described by a log-normal distribution. The negative binomial distribution gives a less satisfactory fit. On comparison with data obtained at lower centre-of-mass energies we observe that KNO scaling is valid in the energy range between 29 and 91.25 GeV. Both QCD (MLLA+LPHD) and a random cascading model give a successful parametrization of the mean charged multiplicity as function of \sqrt{s} . The latter model also successfully predicts the energy dependence of the width of the multiplicity distribution. The width of the distribution is found to be sensitive to higher than next-to-leading order QCD or non-perturbative effects.

Acknowledgements

It is a pleasure to thank our colleagues from the SL division for the performance of the LEP machine and the technical staff of CERN and the home institutes for their contributions to ALEPH. Those of us from non-member states wish to thank CERN for its hospitality.

References

- [1] Z. Koba, H.B. Nielsen, P. Olesen *Nucl. Phys.* **B40** (1972) 317.
- [2] E.D. Malaza, B.R. Webber, *Phys. Lett.* **B149** (1984) 501;
E.D. Malaza, B.R. Webber, *Nucl. Phys.* **B267** (1986) 702.
- [3] S. Carius, G. Ingelman, *Phys. Lett.* **B252** (1990) 647.
- [4] R. Szwed, G. Wrochna, *Z. Phys.* **C47** (1990) 447;
R. Szwed, G. Wrochna, A.K. Wróblewski, *Modern Physics Letters* **A5** (1990) 981.
- [5] ALEPH Collaboration, D. Decamp et al., *Nucl. Inst. & Methods* **A294** (1990) 121.
- [6] UA5 Collaboration, R.E. Ansorge et al., CERN-EP/88-172, Dec.1988;
SFM Collaboration, A. Breakstone et al., *Nuovo Cimento* **102A** (1989) 1199.
- [7] M. Bengtson, T. Sjöstrand, *Phys. Lett.* **B185** (1987) 435.
- [8] T. Sjöstrand, M. Bengtson, *Comput. Phys. Comm.* **43** (1987) 367.
- [9] TASSO Collaboration, W. Braunschweig et al. *Z. Phys.* **C45** (1989) 193.
- [10] C.E. Shannon, *Bell Systems Tech. J.* **27** (1948) 379;
E.T. Jaynes, *Phys. Rev.* **106** (1957) 620.
- [11] J.E. Shore, R.W. Johnson, *IEEE Trans. Inf. Theory* **IT-26** (1980) 26;
J.E. Shore, R.W. Johnson, *IEEE Trans. Inf. Theory* **IT-29** (1983) 942;
Y. Tikochinsky, N.Z. Tishby, R.D. Levine, *Phys. Rev. Lett.* **52** (1984) 379.
- [12] M. Schmelling, Ph.D. thesis, Dortmund, 1987.

- [13] SFM Collaboration, A. Breakstone et al. *Z.Phys.* **C40** (1988) 207.
- [14] ALEPH Collaboration, D. Decamp et al., *Properties of Hadronic Z Decays and Test of QCD Generators*, to be published.
- [15] G. Marchesini, B.R. Webber, *Nucl. Phys.* **B238** (1984) 1; **B238** (1984) 492;
G. Marchesini, B.R. Webber *Nucl. Phys.* **B310** (1988) 461.
- [16] UA5 Collaboration, G.J. Alner et al., *Phys. Lett.* **B138** (1984) 304.
- [17] R.P.Feynman, *Phys. Rev. Lett* **23** (1969) 1415.
- [18] HRS Collaboration, D.Bender et al., *Phys. Rev.* **D31** (1985) 1.
- [19] DELPHI Collaboration, P. Aarnio et al., CERN-PPE/90-173.
- [20] JADE Collaboration, W. Bartel et al., *Z. Phys.* **C20** (1983) 187.
- [21] OPAL Collaboration, M.Z. Akrawy et al., *Z. Phys.* **C47** (1990) 505;
L3 Collaboration, B. Adeva et al., *Phys. Lett.* **B259** (1991) 199;
PLUTO Collaboration, C. Berger et al., *Phys. Lett.* **B95** (1980) 313;
TOPAZ Collaboration, M. Yamauchi et al., Proceedings of the XXIV International Conference on High Energy Physics, p.852 ff.
- [22] W.Thome et al., *Nucl. Phys.* **B129** (1977) 365.
- [23] C.P. Fong and B.R. Webber, Cavendish-HEP-90/2;
Z. Kunszt, P. Nason, G. Marchesini and B.R. Webber, *QCD*, in *Z Physics at LEP*, eds. G. Altarelli, R. Kleiss and C. Verzegnassi, CERN Report 89-08, p. 434 ff.
- [24] Particle Data Group, *Phys. Lett.* **B239** (1990) III.51.
- [25] ALEPH Collaboration, D. Decamp et al., *Phys. Lett.* **B257** (1991) 479.

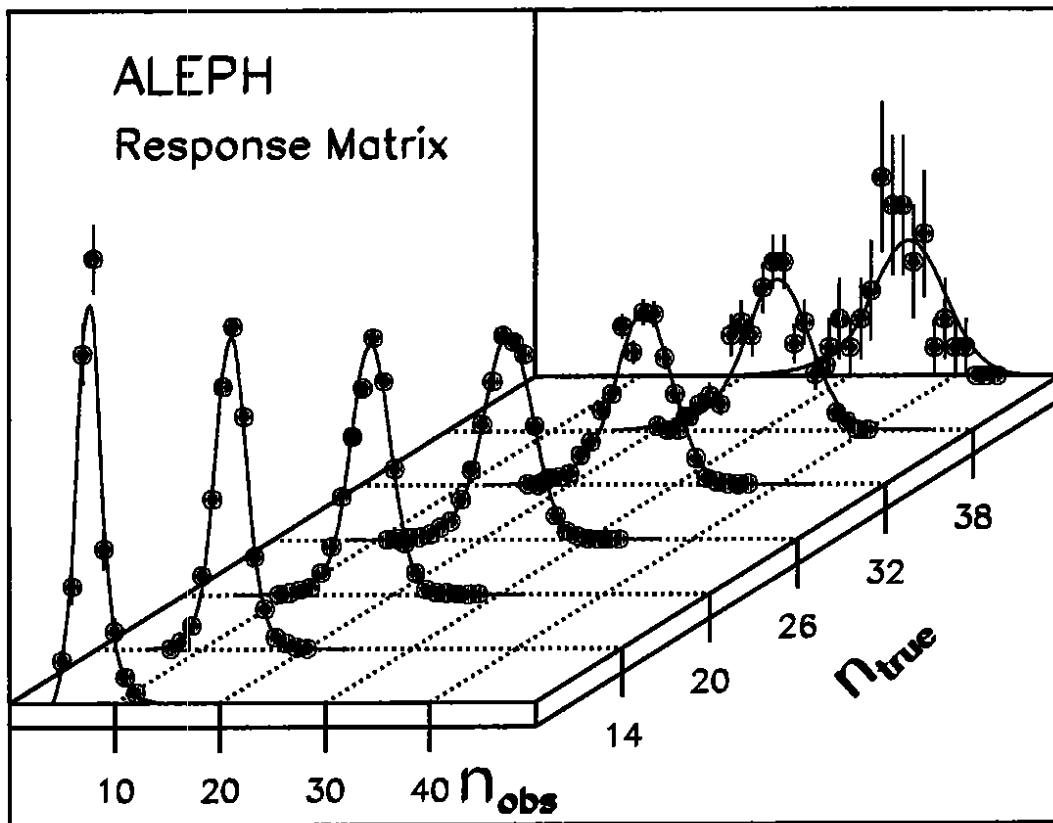


Figure 1: Display of slices of the response matrix: for fixed values of the true charged multiplicity the predicted distribution is shown together with the parametrization of the response matrix.

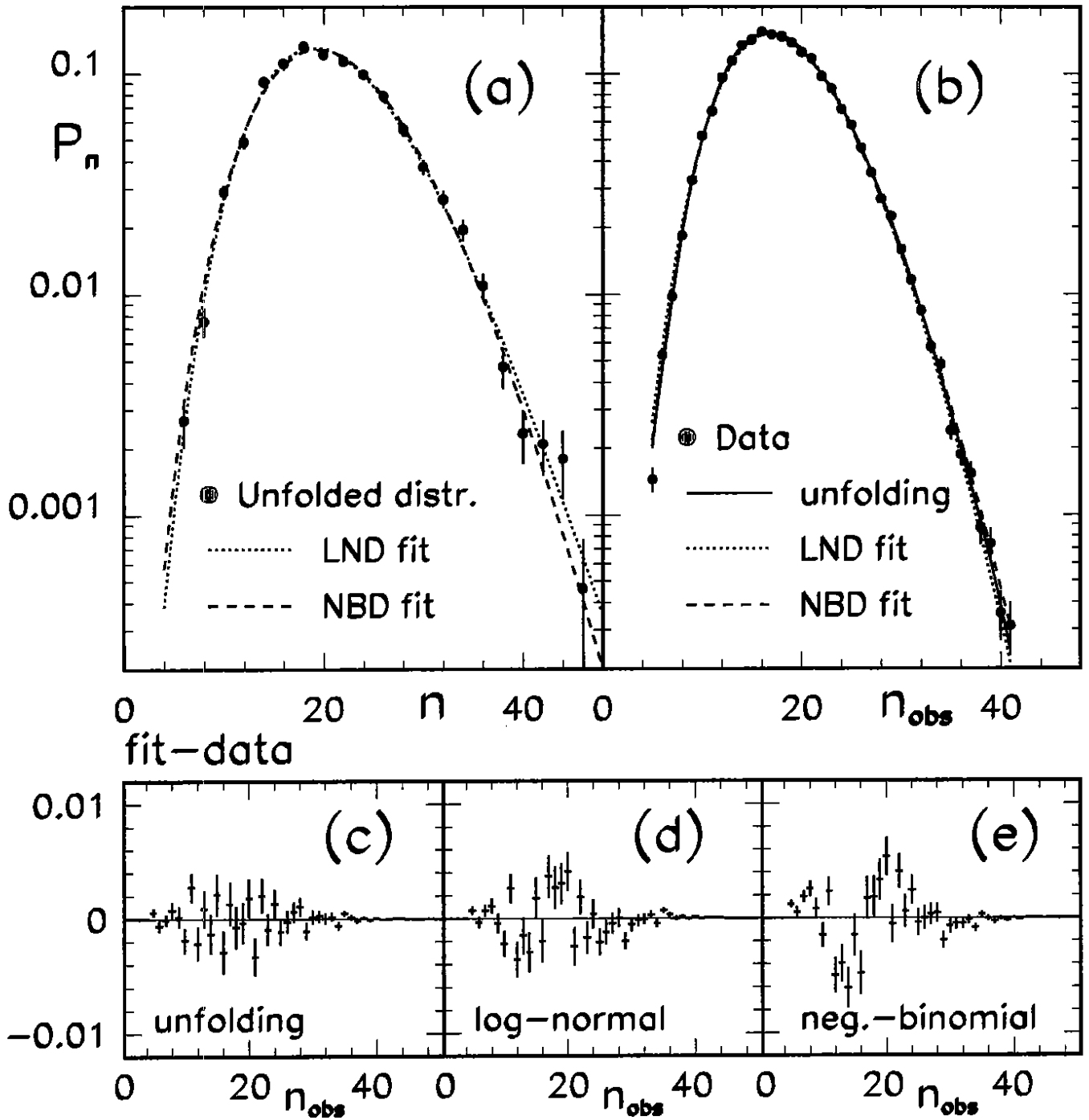


Figure 2: (a) the unfolded charged multiplicity distribution with fits of a log-normal (dotted line) and negative-binomial (dashed line) shape; (b) the comparison of data and all three estimates for the true distribution after convolution with the response matrix; and (c-e) the residuals from (b). The errors are the purely statistical errors of the data.

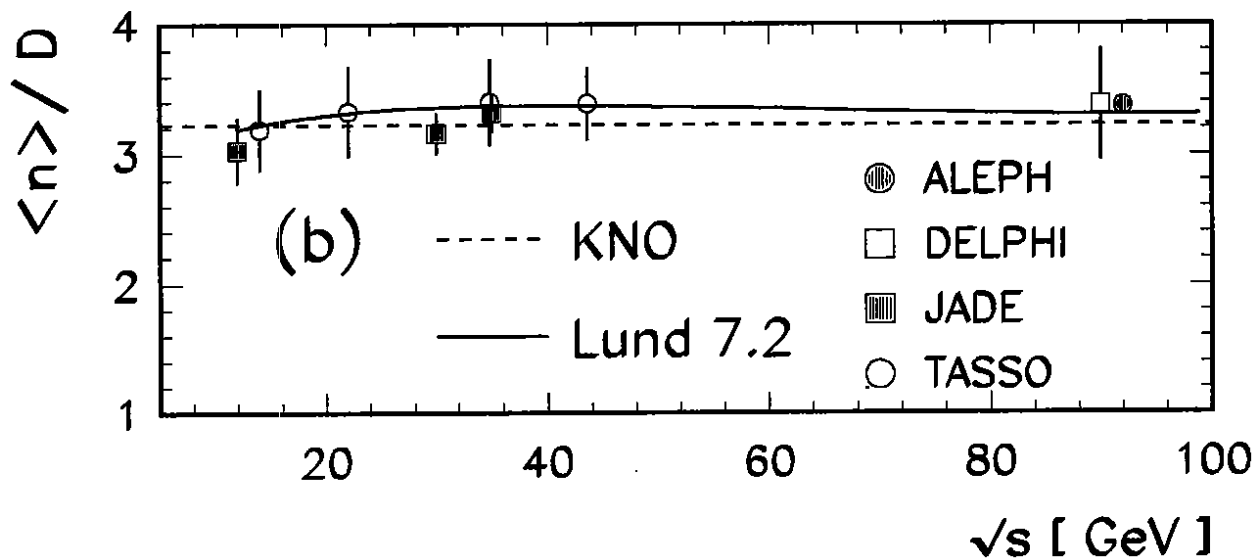
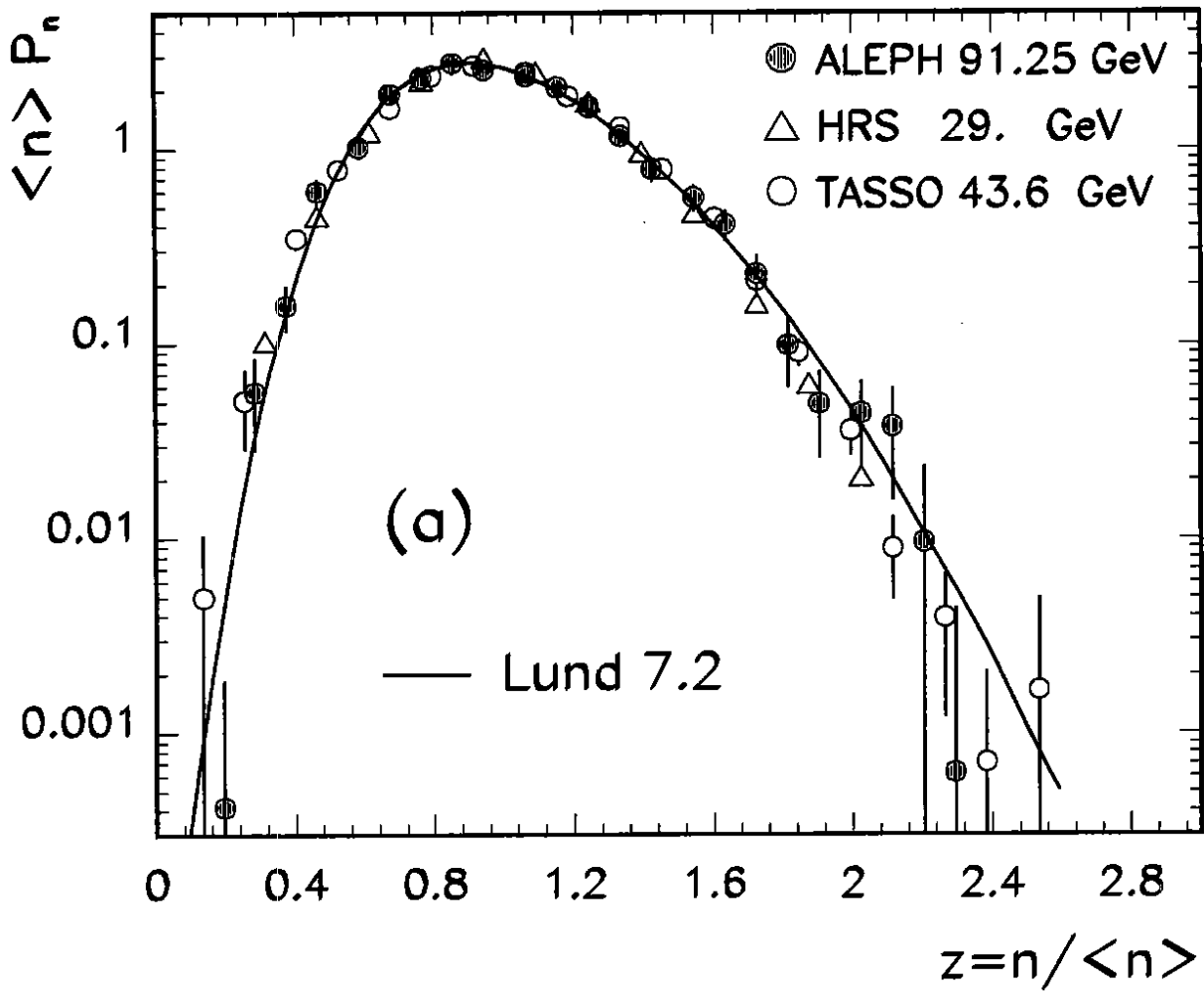


Figure 3: The unfolded charged particle multiplicity distribution in KNO form (a) compared with results from the TASSO and HRS collaboration, and (b) the energy dependence of the ratio $\langle n \rangle / D$. Also shown are the predictions from the Lund 7.2 parton shower model with parameters tuned at $\sqrt{s} = 91.25$ GeV.

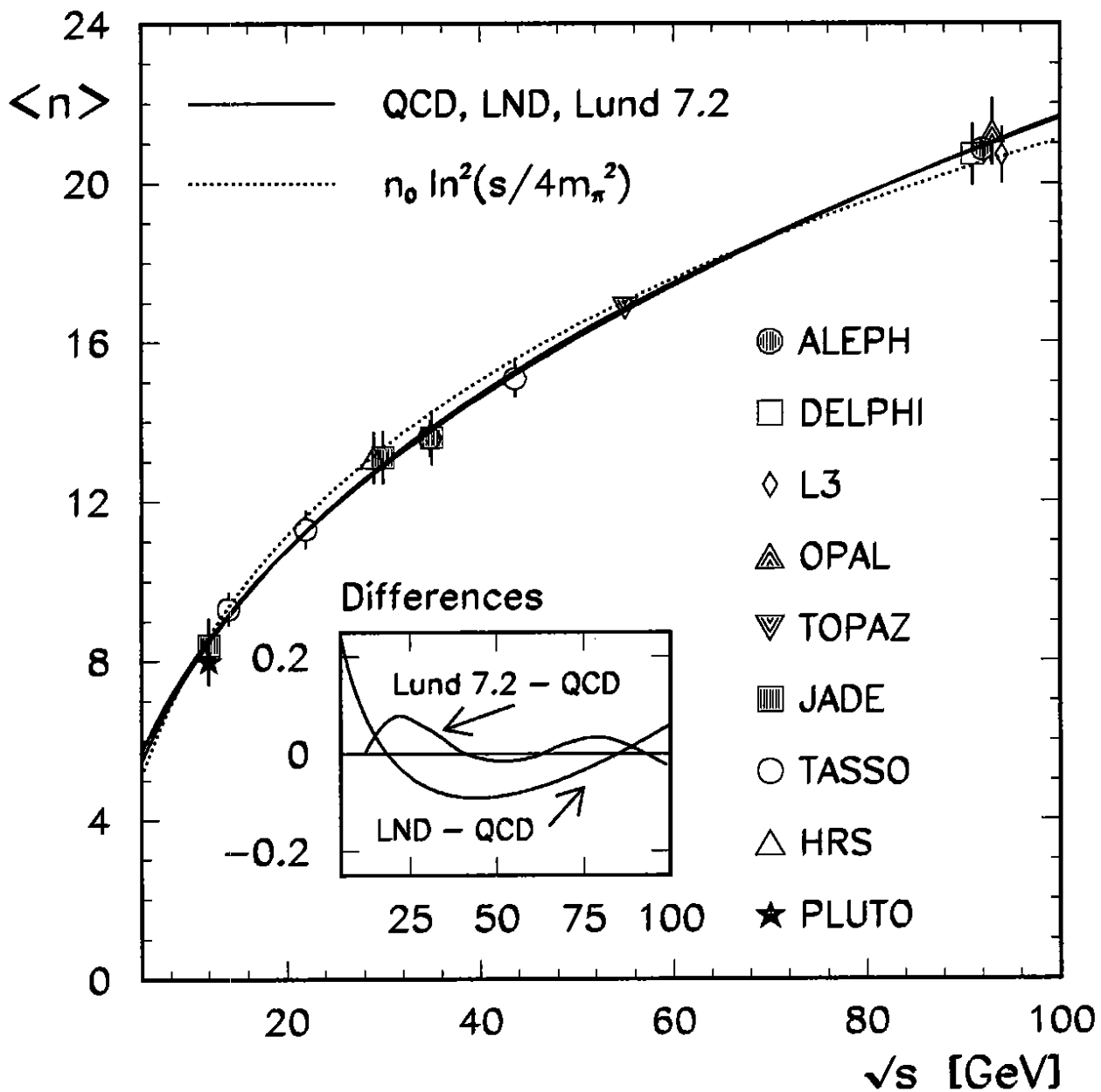


Figure 4: The energy dependence of the mean charged multiplicity compared with a phenomenological parametrization (dotted line), and (full lines) the expectations for a log-normal distribution (LND), the next-to-leading order QCD (MLLA+LPHD) prediction and the prediction from the Lund 7.2 parton shower model. The inset is a blow up of the differences between the QCD curve, Lund 7.2 and LND.

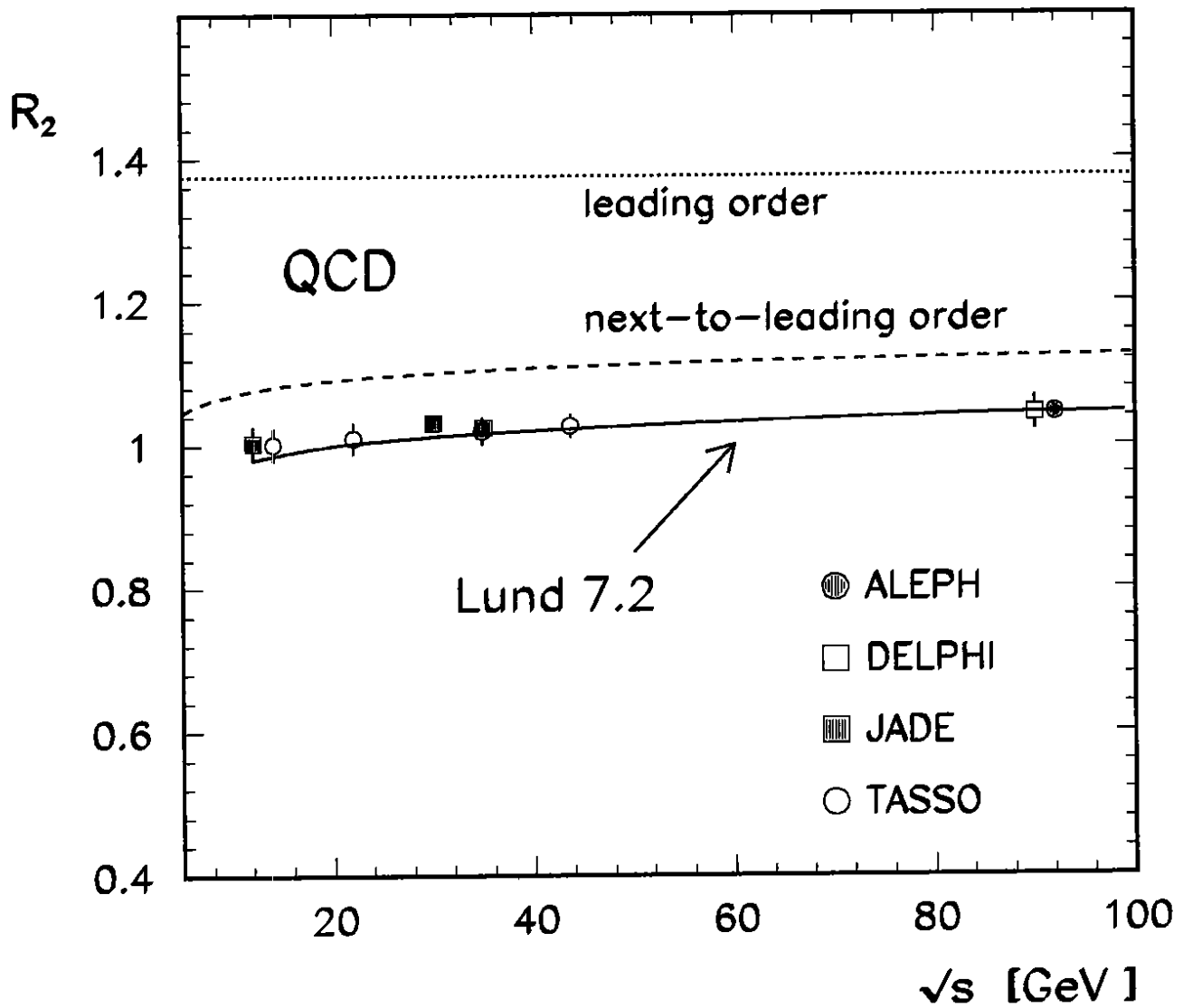


Figure 5: The energy dependence of the second binomial moment compared with the leading (dotted line) and next-to-leading order (dashed line) QCD (MLLA+LPHD) prediction for $\Lambda_{LLA} = 0.145$ GeV. The full line is the prediction from the tuned Lund 7.2 parton shower model.